

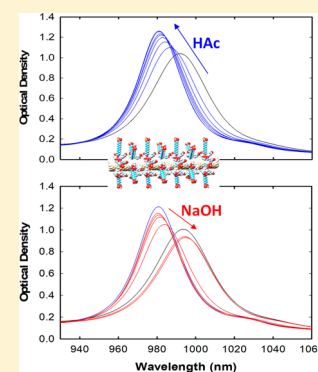
# Selective Protonation of Unbounded Sodium Cholates for Reversible Blue-Shift Absorption Spectra of Single-Chirality Single-Walled Carbon Nanotube in Solution

Huaping Li,\*<sup>1</sup> Lili Zhou, and Nathan K. Smolinski

Atom Optoelectronics 440 Hindry Avenue, Unit E, Inglewood California 90301, United States

## Supporting Information

**ABSTRACT:** In contradiction to the long-standing optical depletion of single-walled carbon nanotubes (SWCNT) by acid doping, this work reports the blue-shifted and optical density-increased  $S_{11}$  (the first Van Hove singularity transition) peak absorption spectra of single-chirality (6,5) SWCNT dispersed in specific surfactant compositions such as 1% SDS (sodium dodecyl sulfate) /1% SC (sodium cholate) and 2% SDS/0.5% SC, which were caused by addition of acid. These anomalous optical changes can be reversed by adding base, and they are discussed on the basis of surfactant arrangements on SWCNT sidewalls, which arose from the selective protonation of unbounded SC to shift the thermodynamic equilibrium of SC adsorbed SWCNT to the desorption of SC from SWCNT surface. The spectroscopic interpretation obeys the dipole moment transition related energy level variation and oscillator strength change.



## INTRODUCTION

With sharp spectrum features near the infrared region, single-chirality single-walled carbon nanotubes (SWCNTs) have been utilized as optical probes for bioimaging and biosensing applications.<sup>1,2</sup> The band gap optical properties of SWCNTs are very sensitive to the adsorbed molecules (including dispersing agents and  $O_2$ ),<sup>3–15</sup> solution media (including pH and ionic strength),<sup>16–23</sup> and environment effects such as temperature and pressure.<sup>23–28</sup> Understanding photophysical properties of SWCNT is critical to precisely interpret the spectroscopic results.

SWCNTs are highly hydrophobic macromolecules that need to be dispersed in solvents using surfactants or polymers for manipulation and practical applications.<sup>29</sup> The measured optical spectral shifts of SWCNTs dispersed in different solvents are reported to scale with their dielectric constants.<sup>30</sup> The effective dielectric constant surrounding SWCNTs depends on their unknown surface coverages of the surfactants.<sup>31</sup> The local dielectric constant is a dielectric superposition of the adsorbed surfactants and incorporated solvents. In this theoretical interpretation, SWCNTs are commonly considered highly polarizable macromolecules with zero net dipole moment. In polar solvents, the dipole induced polarization difference before and after optical excitation was quantified using Onsager polarity function,  $f(\epsilon, \eta) = 2(\epsilon - 1)/(2 \times \epsilon + 1) - 2(\eta - 1)/(2 \times \eta + 1)$ , where  $\epsilon$  and  $\eta$  are the solvent dielectric constant and the reflective index, respectively.<sup>30</sup> In nonpolar solvents, photoexcited SWCNT polarization can induce dynamic polarization of a solvent. The spectral shift was correlated to solvent-induction polarization function  $f(\eta^2) = (\eta^2 - 1)/(2\eta^2 + 1)$  for

interactions between photoexcited SWCNT polarization and polarized solvents.<sup>32</sup>

Recently, we revealed that the optical spectral shifts of single-chirality (6,5) SWCNT in aqueous solution are related to the geometric morphologies and compositions of surfactants (sodium dodecyl sulfate, SDS and sodium cholate, SC) on SWCNT sidewalls.<sup>33</sup> With different geometric morphologies and compositions, the surface areas of (6,5) SWCNT exposed to polar solvents varied and their absorption spectra shifted accordingly. With full coverage of different sole surfactants, different hydration layers were formed around sidewalls of SWCNTs, leading to the differentiated spectral shifts. These results are well consistent with the classic solvatochromic theory in polar solvents.<sup>34,35</sup> Generally, photoexcited SWCNT is polarized to carry photoinduced dipole moments that can be correlated to the optical density of SWCNT absorbance (oscillator strength of exciton,  $f \propto |D|^2$ ,  $D$  is the induced dipole vector). The energy state of polarized SWCNT is more stable when more sidewall surfaces are exposed to a polar solvent, which results in a more red-shifted absorption spectrum.<sup>25</sup> Because of the slow movement of a solvent nuclear part, the solvent electron cloud is also polarized by polarized SWCNT (Franck–Condon effect). The polarized solvent electron cloud exerts back to the polarized SWCNT. These interpolarization processes continue until an equilibrium state is reached. The degree of dipole of initially photoexcited SWCNT reduces during these interpolarization processes. Accordingly, the

Received: November 5, 2018

Revised: January 3, 2019

Published: January 9, 2019

oscillator strength  $f$  (optical density in absorption spectrum) of SWCNT decreases. Additionally, the symmetry of surfactant morphology plays certain roles in spectral changes. For instance, the polarized SWCNT is preferred in surfactant arrangements with low symmetry rather than high symmetry because high symmetrical ground state SWCNT transits to low symmetric photoexcited SWCNT. Thus, the polarized SWCNT in low symmetric surfactant coverage should have lower free Gibbs energy, with peak absorption appearing at longer wavelength than that in high symmetric surfactant encapsulation. The dipole moment transition of photoexcited SWCNT (oscillator strength of absorption) in low symmetric surfactant coverage should be smaller than that in high symmetric surfactant encapsulation.

Since Smalley's research group reported the diminished absorption features of SDS dispersed HiPCO SWCNTs in acid solution,<sup>21</sup> those bleached absorbances were demonstrated to be reversed either by degassing solution<sup>21,36</sup> or using dispersing agents (for examples, SC<sup>37</sup> and dodecyl tethered flavin mononucleotide<sup>38</sup>) that can isolate oxygen from the surfaces of SWCNTs. This acid caused decrease of SWCNTs absorption is generally considered as acid doping, which ignores the changes of SWCNT surface dielectric constant, morphology and symmetry. In this contribution, we report that the diverse absorption spectral changes of (6,5) SWCNT aqueous solution upon addition of acid were observed in various surfactant compositions. For (6,5) SWCNT with more sidewall surface areas exposed to water molecules, their absorption spectra generally shifted to the blue with increasing optical densities by adding acid, and saturated at the points where the surfactant arrangements were finalized. These spectral changes were reversibly recovered by adding base to neutralize the solution. We ascribe these observed spectral changes to reversibly and competitively thermodynamic exchanges of SDS and SC moieties on SWCNT sidewalls, which were tailored by the acidity of aqueous solutions. For the SWCNT with less sidewall surface areas exposed to water molecules or fully covered with sole surfactants, their absorption spectra exhibited surfactant-dependent optical density decreases, similar to those reported protonations of SWCNT by acid doping.<sup>21–23</sup>

## EXPERIMENTAL SECTION

**Materials.** Sodium dodecyl sulfate (SDS) and sodium cholate (SC) were purchased from Sigma-Aldrich and used as received. Sephacryl gel S200 was purchased from GE health. Single-walled carbon nanotubes (SWCNTs) raw powder was produced by Rice University Mark III high pressure carbon monoxide reactor using less catalyst in a yield of 1 g per hour. Acetic acid (5%, 0.833 mol/L), HCl (3.65%, 1.0 mol/L) and NaOH (3.32%, 0.83 mol/L) were used as acids and base, respectively. The raw SWCNTs were used for the extraction of (6,5) SWCNT using gel permeation chromatography. The (6,5) SWCNT stock solutions dispersed in 5% SDS, 2% SDS, 2% SDS/0.05% SC, 2% SDS/0.5% SC, 1% SDS/1% SC, and 5% SC were obtained by eluting the trapped (6,5) SWCNT in Sephacryl gels with according surfactant compositions. All concentration units are weight percentage unless there are specific descriptions.

**Measurements.** All visible near-infrared absorption spectra of (6,5) SWCNT dispersed in different surfactant systems were measured on a NS3 Applied Nano Spectralyzer at ambient

temperature. The optical path length is 1 cm. The starting solution volumes are 1 mL.

## RESULTS AND DISCUSSION

With the sharp absorbance of the first Van Hove singularity transition ( $S_{11}$ ), the single-chirality (6,5) SWCNT extracted from high pressure CO conversion carbon nanotubes can be employed as the optical probe without the need of spectral deconvolution.<sup>39,40</sup> In this contribution, the diverse  $S_{11}$  absorbance changes of (6,5) SWCNT dispersed in aqueous solutions with various surfactant compositions (sodium dodecyl sulfate (SDS), sodium cholate (SC)) were investigated. Their chemical structures are illustrated in Supporting Information, Figure S1. The visible near-Infrared absorption spectra of (6,5) SWCNT dispersed in 5% SDS (pH = 7.6), 2% SDS (pH = 7.4), 2% SDS/0.05% SC (pH = 8.0), 2% SDS/0.5% SC (pH = 8.5), 1% SDS/1% SC (pH = 8.7), and 5% SC (pH = 9.0) were measured using NS3 Applied Nano Spectralyzer (Supporting Information, Figure S2). To elucidate the spectral shift, the measured absorption spectra were normalized at  $S_{11}$  peak absorbances and presented in Figure 1A. Their  $S_{11}$  peak wavelengths were plotted against different

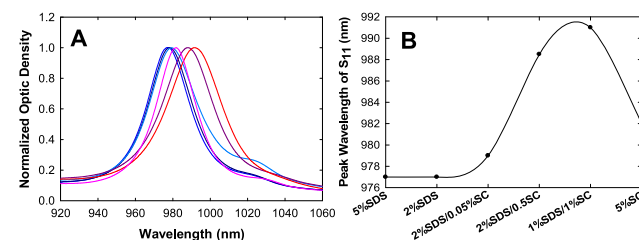


**Figure 1.** (A) Normalized  $S_{11}$  absorption spectra of (6,5) SWCNT dispersed in 5% SDS (blue curve), 2% SDS (dark blue curve), 2% SDS/0.05% SC (light blue curve), 2% SDS/0.5% SC (dark red curve), 1% SDS/1% SC (red curve), and 5% SC (pink curve). (B) Plot of  $S_{11}$  peak wavelengths of (6,5) SWCNT against different surfactant compositions in which (6,5) SWCNT was dispersed.

surfactant compositions (Figure 1B). Clearly, the  $S_{11}$  peak absorption of (6,5) SWCNT dispersed in 5% SDS and 2% SDS appears at 977 nm, 2% SDS/0.05% SC at 979 nm, 2% SDS/0.5% SC at 989 nm, 1% SDS/1% SC at 991 nm, and 5% SC at 982 nm, respectively. A minor peak located at 1030 nm could be due to other SWCNT with different chirality, such as (10,2). The  $S_{11}$  peak absorption of (6,5) SWCNT dispersed in high concentration SDS (2% and 5%) occurred at the bluest region. When SC was introduced to (6,5) SWCNT dispersed in high concentration SDS solution, the  $S_{11}$  peak absorption of (6,5) SWCNT started shifting to the red. A larger shift was observed with more SC, i.e., the  $S_{11}$  peak absorption of (6,5) SWCNT dispersed in 2% SDS/0.5% SC is at the red site of that of (6,5) SWCNT dispersed in 2% SDS/0.05% SC. The redshift of (6,5) SWCNT dispersed in 1% SDS/1% SC reached an upper limit. The  $S_{11}$  peak absorption of (6,5) SWCNT dispersed in high concentration SC (5%) shifted back to blue, between those of (6,5) SWCNT dispersed in 2% SDS/0.5% SC and 2% SDS/0.05% SC. These results are consistent with our reported spectral changes of (6,5) SWCNT dispersed in 2% SDS titrated with SC.<sup>33</sup> These spectral variations thus can be interpreted using our previous hypothesis.<sup>33</sup> In high concentration SDS solutions (5% SDS and 2% SDS), rod-like micelles of SDS around (6,5) SWCNT were formed. One SC

moiety replaced the corresponding SDS rod-like segment to open SWCNT surface to water molecules, leading to the red-shifted  $S_{11}$  absorbance of (6,5) SWCNT. More SC molecules can supersede more segments of rod-like SDS micelles to expose more SWCNT surfaces to water solvent with the more red-shifted  $S_{11}$  absorption spectra. Likely, (6,5) SWCNT dispersed in 1% SDS/1% SC has maximal surfaces exposure to water molecules, showing the maximally red-shifted  $S_{11}$  peak absorption. With high concentrated SC, the SC micelles with rigid helix structures were formed around SWCNT sidewalls, having limited surface areas open to polar water media, less than the opened surface areas of SWCNTs dispersed in 2% SDS/0.5% SC, but more than those of SWCNTs dispersed in 2% SDS/0.05% SC.

The absorption spectra of (6,5) SWCNT dispersed in 1% SDS/1% SC (1 mL solution) were measured upon addition of 0  $\mu\text{L}$  (pH = 8.7), 1  $\mu\text{L}$  (pH = 3.9), 2  $\mu\text{L}$  (pH = 3.8), 3  $\mu\text{L}$  (pH = 3.8), 4  $\mu\text{L}$  (pH = 3.6), 5  $\mu\text{L}$  (pH = 3.6), 7  $\mu\text{L}$  (pH = 3.5), 10  $\mu\text{L}$  (pH = 3.4), 15  $\mu\text{L}$  (pH = 3.4), 20  $\mu\text{L}$  (pH = 3.3) of 5% HAc (Supporting Information, Figure S3). Their  $S_{11}$  absorbance spectra are exhibited in Figure 2A. Their  $S_{11}$

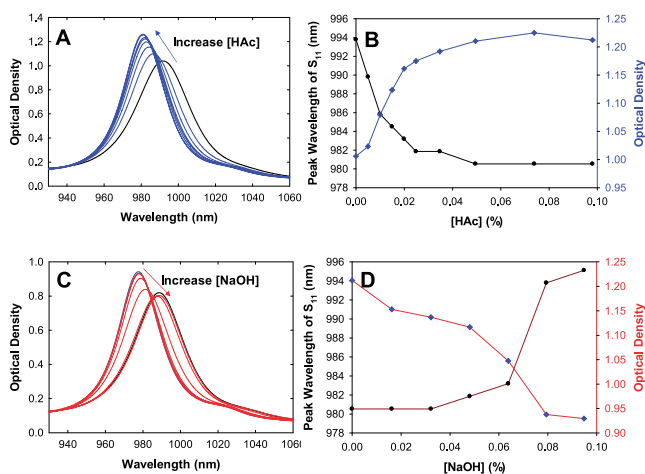


**Figure 2.** (A)  $S_{11}$  absorption spectra of (6,5) SWCNT dispersed in 1% SDS/1% SC upon addition of 5% HAc in volumes of 0 (black curve), 1, 2, 3, 4, 5, 7, 10, 15, and 20  $\mu\text{L}$  (blue curves). (B) Plots of  $S_{11}$  peak wavelengths (black curve) and  $S_{11}$  peak optical density (blue curve) against the concentrations of HAc. (C)  $S_{11}$  absorption spectra of (6,5) SWCNT dispersed in 1% SDS/1% SC (black curve), after addition of 20  $\mu\text{L}$  of 5% HAc (blue curve), and after addition of 3.32% NaOH in volumes of 5, 10, 15, 20, 25, and 30  $\mu\text{L}$  (red curves). (D) Plots of  $S_{11}$  peak wavelengths (dark red curve) and  $S_{11}$  peak optical density (red curve) against the concentrations of NaOH.

peak wavelengths (black curve) and optical densities (blue curve) are plotted against the concentrations of HAc as shown in Figure 2B. The results show the  $S_{11}$  peak absorption wavelength shifted from 981 nm and the  $S_{11}$  peak optical density increased from 1.00 to 1.21 when 5% HAc was added from 1 to 20  $\mu\text{L}$ . The  $S_{11}$  peak wavelength of (6,5) SWCNT remained constant at 981 nm after the addition of 10  $\mu\text{L}$  or more of 5% HAc. The optical density of  $S_{11}$  peak absorption reached a maximum after the addition of 15  $\mu\text{L}$  of 5% HAc, then slightly decreased with further addition of 5% HAc. These spectral changes were reversed by adding various volumes of 3.3% NaOH. The absorption spectra of (6,5) SWCNT dispersed in 1% SDS and 1% SC added with 20  $\mu\text{L}$  of 5% HAc were measured by further addition of 3.3% NaOH in

5  $\mu\text{L}$  (pH = 3.4), 10  $\mu\text{L}$  (pH = 3.4), 15  $\mu\text{L}$  (pH = 3.6), 20  $\mu\text{L}$  (pH = 8.7), 25  $\mu\text{L}$  (pH = 11.6), and 30  $\mu\text{L}$  (pH = 11.9) (Supporting Information, Figure S4). Their  $S_{11}$  absorption spectra are shown in Figure 2C and the plots of their  $S_{11}$  peak wavelengths (dark red curve) and  $S_{11}$  peak optical densities (red curve) against the concentrations of NaOH are presented in Figure 2D. The results unambiguously display that the  $S_{11}$  peak absorption wavelength of (6,5) SWCNT shifted back from 981 to 995 nm, and their  $S_{11}$  peak optical densities decreased from 1.21 to 0.93.

The similar spectral changes were observed for (6,5) SWCNT dispersed in 2% SDS/0.5% SC (pH = 8.5), but with reduced amplitudes. The measured absorption spectra of (6,5) SWCNT dispersed in 2% SDS/0.5% SC upon the addition of 5% HAc are shown in Supporting Information, Figures S5 and S6. Their  $S_{11}$  absorption spectra are exhibited in Supporting Information, Figures S7A and S8A respectively. The plots of their  $S_{11}$  peak wavelengths and optical densities against the added volume of 5% HAc were plotted in Supporting Information, Figures S7B and S8B. The reproducible results show the  $S_{11}$  peak wavelength of (6,5) SWCNT dispersed in 2% SDS/0.5% SC (pH = 8.5) shifted from 989 to 977.5 nm upon addition of 15  $\mu\text{L}$  (pH = 3.4) of 5% HAc. The  $S_{11}$  peak wavelength of (6,5) SWCNT remained constant after addition of 5  $\mu\text{L}$  (pH = 3.6) of 5% HAc. The maximal optical density of  $S_{11}$  peak absorbance was reached upon addition of 10  $\mu\text{L}$  (pH = 3.4) of 5% HAc and then slightly decreased upon further addition of 5% HAc. The reversed absorption spectra of (6,5) SWCNT dispersed in 2% SDS/0.5% SC were also observed upon addition of 3.3% NaOH in 2  $\mu\text{L}$  (pH = 3.4), 4  $\mu\text{L}$  (pH = 3.4), 6  $\mu\text{L}$  (pH = 3.5), 8  $\mu\text{L}$  (pH = 3.5), 10  $\mu\text{L}$  (pH = 3.6), and 12  $\mu\text{L}$  (pH = 3.8) (Supporting Information, Figure S9). Their  $S_{11}$  absorption spectra are shown in Supporting Information, Figure S10A and the plots of their  $S_{11}$  peak wavelengths and  $S_{11}$  peak optical densities against the added volumes of 3.3% NaOH are presented in Figure S10B. The  $S_{11}$  peak wavelength of (6,5) SWCNT shifted from 978 nm back to 989 nm when 12  $\mu\text{L}$  of 3.3% NaOH was added. Simultaneously, their peak optical densities decreased back to their original peak optical density (slightly lower than the starting absorption spectrum).

HAc is a weak organic acid. To rule out organic solvent effect, 3.65% HCl was used as the substitute for 5% HAc.<sup>15</sup> The absorption spectra of (6,5) SWCNT dispersed in 2% SDS/0.5% SC (pH = 8.5) were measured upon addition of 1  $\mu\text{L}$  (pH = 3.0), 2  $\mu\text{L}$  (pH = 2.7), 3  $\mu\text{L}$  (pH = 2.5), 4  $\mu\text{L}$  (pH = 2.4), and 5  $\mu\text{L}$  (pH = 2.3) of 3.65% HCl and then 2  $\mu\text{L}$  (pH = 2.4), 4  $\mu\text{L}$  (pH = 2.9) and 6  $\mu\text{L}$  (pH = 3.2) of 3.3% NaOH, sequentially (Supporting Information, Figure S11). Their  $S_{11}$  absorption spectra are presented in Figure 3A, blue curves for addition of HCl and red curves for addition of NaOH. The plots of  $S_{11}$  peak wavelengths and optical densities against the concentrations of 3.65% HCl (bottom coordinate) and of NaOH (top coordinate) are shown in Figure 3B. The plots show  $S_{11}$  peak wavelength of (6,5) SWCNT dispersed in 2% SDS/0.5% SC shifted from 988.5 to 978 nm after addition of 15  $\mu\text{L}$  of 3.65% HCl, and then reversed back to 989 nm after addition of 12  $\mu\text{L}$  (in total) of 3.32% NaOH. The  $S_{11}$  peak optical densities of (6,5) SWCNT dispersed in 2% SDS/0.5% SC increased from 0.77 to 0.89 after addition of 15  $\mu\text{L}$  of 3.65% HCl and reversed back to 0.77 after addition of 12  $\mu\text{L}$  (in total) of 3.32% NaOH.

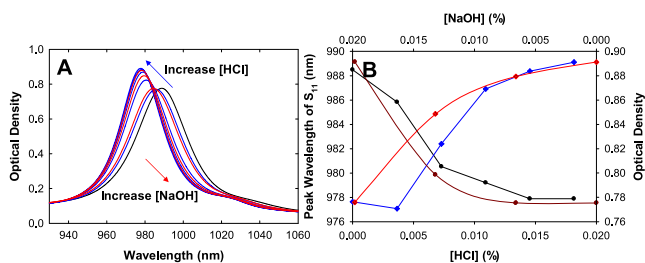
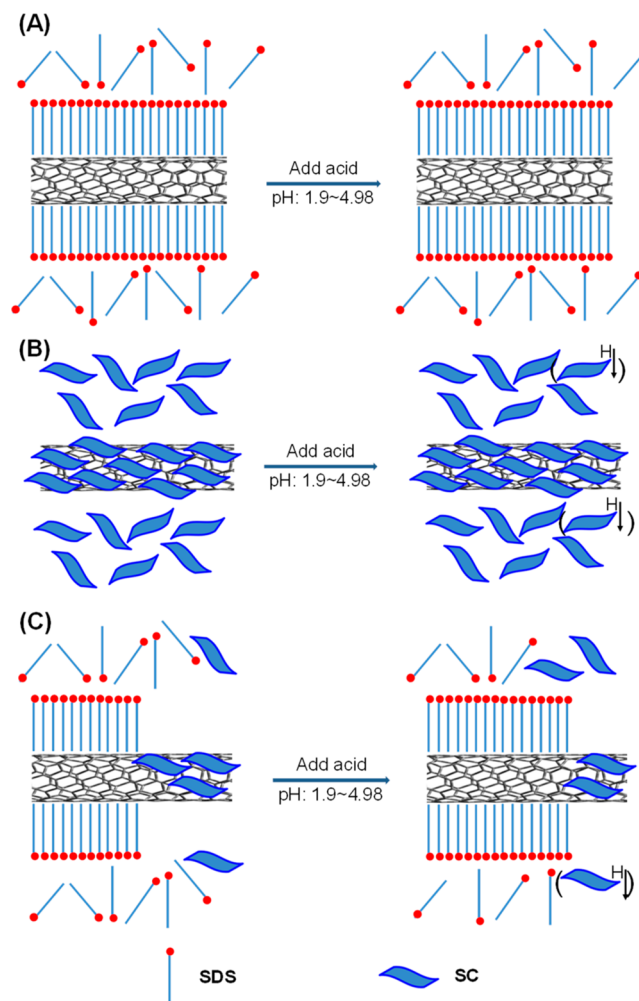


**Figure 3.** (A)  $S_{11}$  absorption spectra of (6,5) SWCNT dispersed in 2% SDS/0.5% SC upon addition of 3.65% HCl in volumes of 0 (black curve), 1, 2, 3, 4, and 5  $\mu\text{L}$  (blue curves) and addition of 3.32% NaOH in volumes of 2, 4, and 6  $\mu\text{L}$  (red curves). (B) Plots of  $S_{11}$  peak wavelengths (black curve) and  $S_{11}$  peak optical density (blue curve) against the concentrations of HCl (bottom coordinate) and plots of  $S_{11}$  peak wavelengths (dark red curve) and  $S_{11}$  peak optical density (red curve) against the concentration of NaOH (top coordinate).

These results show these blue-shifted and optical density increased  $S_{11}$  absorption spectra of (6,5) SWCNT dispersed in 1% SDS/1% SC and 2% SDS/0.5% SC upon addition of acids (either HAc or HCl) are reproducible and consistent phenomenon, and can be reversed back after addition of a base (NaOH). Interestingly, the  $S_{11}$  absorption spectra of (6,5) SWCNT dispersed in 1% SDS/1% SC and 2% SDS/0.5% SC implied that SWCNT surface areas exposure to water environment approach to their maxima. On the basis of our previous spectral dilution and titration studies of (6,5) SWCNTs in different surfactants<sup>33</sup> and well-known solvatochromic effects on SWCNTs absorption spectra,<sup>30–32</sup> we rationalize these blue-shifted  $S_{11}$  absorption spectra of (6,5) SWCNT to the surfactant reorganization induced by addition of acid that mitigated SWCNT sidewall surface areas exposure to water molecules. The  $\text{pK}_a$  values of HAc, dodecyl sulfuric acid, cholic acid are 4.8,<sup>41</sup> 1.9<sup>42</sup> and 4.98<sup>43</sup> respectively. With  $\text{pH} > 1.9$ , SDS will not be protonated. Likely, SC will be protonated when  $\text{pH}$  value reaches 5 or less.<sup>44</sup> For example, the cloudy solution appeared when 10  $\mu\text{L}$  of 5% HAc was injected into (6,5) SWCNT dispersed in 5% SC solution, implying the protonation of SC moieties (Supporting Information, Figure S12). SDS adsorbed on SWCNT should have the  $\text{pK}_a$  value similar to that of the free SDS molecule based on their similar  $\zeta$  potential values.<sup>45</sup> SC adsorbed on SWCNT could have  $\text{pK}_a$  value much smaller than that of free SC molecule because SC dispersed SWCNT solution has about 28 mV more negative  $\zeta$  potential in comparison to SC without SWCNT.<sup>46</sup> On the basis of these analyses, the addition of enough acid (either of HAc or HCl), free SC molecules would selectively be protonated and form aggregates in aqueous solution (Scheme 1). Additionally, the critical micelle concentration of SC would decrease with the protonation of SC by adding acid. The reduced free SC moieties then shifted the thermodynamic equilibrium of SC bounded SWCNTs to SC desorption from the SWCNT sidewall. Consequently, SDS molecules from free SDS moieties and SDS micelles would occupy these surface areas and diminish the surface areas exposure to water solvent via molecular exchanges.<sup>33</sup> In this situation, the blue-shifted absorption spectra were observed because of the upraised energy level of polarized SWCNTs in less polar environment. Simultaneously, the dipole moment of a polarized SWCNT was weakly suppressed by a less polar environment in

**Scheme 1. Cartoon Diagrams To Show the Acid Effect on Surfactant Arrangements of (6,5) SWCNT Dispersed in Different Surfactant Compositions<sup>a</sup>**



<sup>a</sup>Key: (A) Highly concentrated SDS (2% and 5%), no protonation for individual SDS or rod-like SDS on SWCNT surface by adding acid with  $\text{pH}$  from 4.98 to 1.9. (B) Highly concentrated SC (5%), with protonation of individual SC but no protonation of SC micelles on SWCNT surfaces by adding acid with  $\text{pH}$  from 4.98 to 1.9. (C) Highly concentrated SDS with SC (2% SDS/0.5% SC and 1% SDS/1% SC), selective protonation of individual SC but no protonation of individual SDS, rod-like SDS on SWCNT surfaces and SC micelles on SWCNT surfaces by adding acid with  $\text{pH}$  from 4.98 to 1.9.

comparison to the strong dipole moment suppression of polarized SWCNT by polar media, leading to the increase of oscillator strength  $f$  of  $S_{11}$  peak absorption. Reversely, deprotonation of cholic acid by adding NaOH base led to the increased concentration of free SC, which in turn competitively substitute SDS adsorbed on SWCNTs through molecular exchanges simply because free SC has stronger binding strength on the SWCNT sidewall than SDS moieties.<sup>33,47,48</sup> Thus, the sidewall surface of the SWCNT was reopened and exposed to polar water solvent, leading to the reversed changes in  $S_{11}$  absorption spectra.

The absorption spectra of (6,5) SWCNT dispersed in 2% SDS/0.05% SC ( $\text{pH} = 8.0$ ), 2% SDS ( $\text{pH} = 7.4$ ), 5% SDS ( $\text{pH} = 7.6$ ) and 5% SC ( $\text{pH} = 9.0$ ) after addition of 5% HAc were measured (Supporting Information, Figures S13–S16). Their

$S_{11}$  absorption spectra are illustrated in parts A, C, E, and G of Figure 4, and the plots of their  $S_{11}$  peak wavelengths and peak

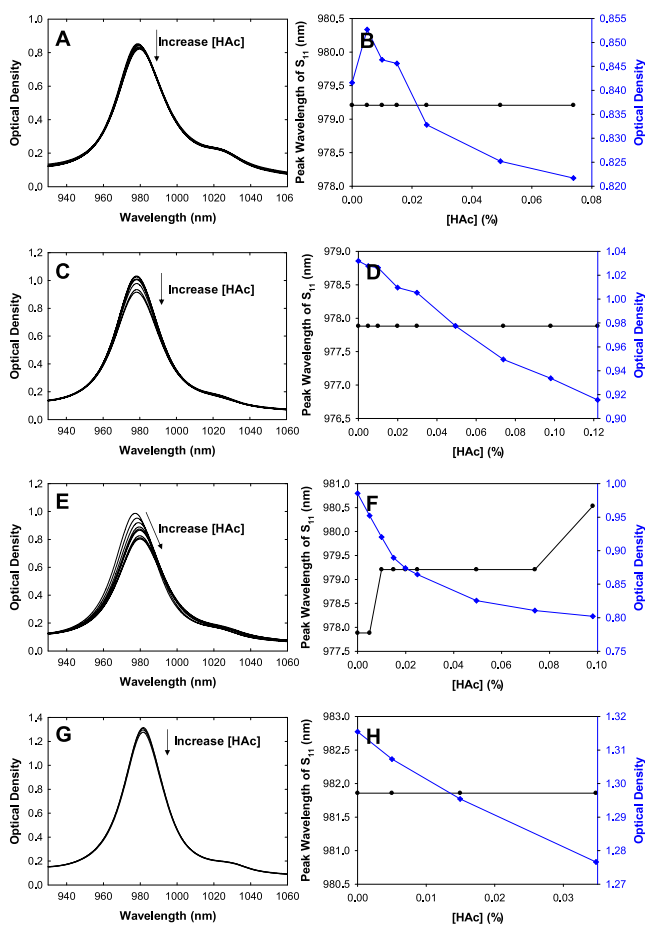


**Figure 4.** (A)  $S_{11}$  absorption spectra of (6,5) SWCNT dispersed in 2% SDS/0.05% SC upon addition of 5% HAc in volumes of 0, 1, 2, 3, 5, 10, and 15  $\mu\text{L}$ . (B) Plots of  $S_{11}$  peak wavelengths (black curve) and  $S_{11}$  peak optical density (blue curve) of (6,5) SWCNT dispersed in 2% SDS/0.05% SC against the concentrations of HAc. (C) The  $S_{11}$  absorption spectra of (6,5) SWCNT dispersed in 2% SDS upon addition of 5% HAc in volumes of 0, 1, 2, 4, 6, 10, 15, 20, and 25  $\mu\text{L}$ . (D) Plots of  $S_{11}$  peak wavelengths (black curve) and  $S_{11}$  peak optical density (blue curve) of (6,5) SWCNT dispersed in 2% SDS against the concentrations of HAc. (E)  $S_{11}$  absorption spectra of (6,5) SWCNT dispersed in 5% SDS upon addition of 5% HAc in volumes of 0, 1, 2, 3, 4, 5, 10, 15, and 20. (F) Plots of  $S_{11}$  peak wavelengths (black curve) and  $S_{11}$  peak optical density (blue curve) of (6,5) SWCNT dispersed in 5% SDS against the concentrations of HAc. (G)  $S_{11}$  absorption spectra of (6,5) SWCNT dispersed in 5% SC upon addition of 5% HAc in volumes of 0, 1, 3, and 7  $\mu\text{L}$ . (H) Plots of  $S_{11}$  peak wavelengths (black curve) and  $S_{11}$  peak optical density (blue curve) of (6,5) SWCNT dispersed in 5% SC against the concentrations of HAc.

optical densities against the concentrations of HAc are presented in parts B, D, F, and H of Figure 4, respectively. Different from these spectral changes of (6,5) SWCNT dispersed in 1% SDS/1% SC and 2% SDS/0.5% SC, their  $S_{11}$  peak absorbances remained constant except for (6,5) SWCNT dispersed in 5% SDS with slightly red-shift upon addition of 5% HAc. Their  $S_{11}$  peak optical densities decreased upon addition of 5% HAc, except for (6,5) SWCNT dispersed in 2% SDS/0.05% SC with a slightly increase in optical density

initially when 1  $\mu\text{L}$  (pH = 3.9) of 5% HAc added. The decreases in amplitudes are significantly different with different surfactant compositions.<sup>37</sup> Here, (6,5) SWCNT dispersed in 5% SDS and 2% SDS showed large decreases in amplitudes of  $S_{11}$  peak optical densities, from 0.98 to 0.80 and from 1.035 to 0.915, respectively. The decreases in amplitudes of the  $S_{11}$  peak optical densities of (6,5) SWCNT dispersed in 5% SC (from 1.316 to 1.276) and 2%SDS/0.05% SC (from 0.842 to 0.822) are relatively small. Consistent with other literature reports,<sup>23,36,37</sup> these declined  $S_{11}$  peak optical densities were restored by adding 3.3% NaOH solution.

For SWCNTs dispersed in 5% SDS (pH = 7.6), 2% SDS (7.4), 2% SDS/0.05% SC (pH = 8.0) and 5% SC (pH = 9.0), their sidewall surface areas exposure to water solvent were constrained and hardly disturbed by addition of acid. No  $S_{11}$  peak wavelength shift was thus observed upon addition of acids. This indicates no perturbation on the equilibrium of SDS and SDS encapsulated SWCNT by adding acids with the eventual pH ranging from 4.98 to 1.9 (Scheme 1A). Although the protonation of unbounded SC moieties theoretically occurred, sufficient amounts of SC molecules still remained in solution, and the conformation of SWCNT wrapped with SC helix structure remained the same (Scheme 1B). These unchanged SWCNT surfaces displayed their nonshifted  $S_{11}$  peak absorption. These observed  $S_{11}$  peak optical density decreases have been interpreted by the protonation of SWCNT sidewall surfaces due to acid doping. The differential decreases in amplitude of the  $S_{11}$  peak absorption of (6,5) SWCNT dispersed in sole SDS or SC may be interpreted by their  $\zeta$  potentials,<sup>45,46</sup> where SC adsorbed SWCNT has more negative  $\zeta$  potential than SDS adsorbed SWCNT to limit the penetration of the added acid. The slightly red-shifted  $S_{11}$  peak wavelengths of (6,5) SWCNT dispersed in 5% SDS could be due to attractive depletion (high concentrated electrolytes induced aggregations leading to red-shifted wavelength and optical density decrease) of nanoscale particles.<sup>37</sup> This kind of  $S_{11}$  peak optical density decrease can be expected to occur for (6,5) SWCNT dispersed in 1% SDS/1% SC and 2% SDS/0.5% SC solutions (actually, the slightly decreased  $S_{11}$  peak optical densities were observed after the maximum  $S_{11}$  peak optical densities were reached upon addition of acids). The obtained results in Figure 2 and Figure 3 imply the spectral changes were dominated by  $S_{11}$  peak optical density increases due to diminished surface areas exposure to water polar media.

With the above-discussed absorption of spectral diversities of (6,5) SWCNT dispersed in various surfactant compositions upon addition of acids, their variabilities to elute SWCNTs trapped in gels were tested. Though the obvious optical changes of (6,5) SWCNT dispersed in 1% SDS/1% SC and 2% SDS/0.5% SC solutions were observed, the eluting strengths of 1% SDS/1% SC and 2% SDS/0.5% SC in gel chromatography using Sephacryl gel 200 as the media were negligibly different upon addition of acids. These eluants might already have strong eluting strengths because of the presence of a significant amount of SC molecules. While no apparent  $S_{11}$  peak wavelength shift was observed for (6,5) SWCNT dispersed in 2% SDS/0.05% SC solution, the strength of 2% SDS/0.05% SC to elute SWCNT was significantly enhanced by addition of acids in gel chromatography using Sephacryl gel 200 as the media.<sup>49</sup> For 2% SDS elution, the maximal eluting strength was observed when 4  $\mu\text{L}$  of 5% HAc (pH = 3.6) was added. More interestingly, loading (6,5) SWCNT dispersed in 0.5% SDS at pH  $\sim$  5 in Saphacryl gel 200, no SWCNT could be trapped in

the gel. Neutralizing (6,5) SWCNT dispersed in 0.5% SDS to pH  $\sim$  7.8 by adding NaOH, the retention of (6,5) SWCNT in Sephacryl gel was obtained. These varied eluting strength changes by adding acids may not seem relevant to the surfactant arrangement on the SWCNT sidewall, which likely arose from the  $\zeta$  potential disparity of different surfactant compositions by addition of acid and base, which led to various electrostatic screening effects that determined the retention of SWCNT in gels.<sup>33,45,46</sup>

## CONCLUSION

In summary, the absorption spectra of (6,5) SWCNT dispersed in a series of surfactant compositions like 5% SDS, 2% SDS, 2% SDS/0.05% SC, 2% SDS/0.5% SC, 1% SDS/1% SC, and 5% SC were measured upon addition of varied amount of acids (either 5% HAc or 3.65% HCl). For these (6,5) SWCNT dispersed in surfactant compositions such as 1% SDS/1% SC and 2% SDS/0.5% SC exhibiting  $S_{11}$  peak absorption in red-shift region (more SWCNT surface areas exposure to water microenvironment), their  $S_{11}$  peak absorption wavelengths were significantly blue-shifted and their  $S_{11}$  peak optical density increased upon addition of acid. These spectral changes were reversed by adding 3.32% NaOH. We conceivably ascribed these optical changes to surfactant rearrangements around a SWCNT sidewall that mitigated the SWCNT surface areas exposure to water molecules triggered by the protonation of free SC moieties. The decreased SC concentration in aqueous solution shifted the thermodynamic equilibrium of SC adsorbed SWCNT to SC desorption from SWCNT sidewall surface, and the desorbed SC moieties were subsequently substituted by SDS moieties. The blue-shifted  $S_{11}$  peak absorption can be explained by the increased energy level of polarized (6,5) SWCNT in a less polar environment, and the increased  $S_{11}$  peak optical density can be credited to the release of suppressed dipole moment of polarized (6,5) SWCNT in polar medium. For these (6,5) SWCNT dispersed in surfactant compositions such as 5% SDS, 2% SDS, 2% SDS/0.05% SC, and 5% SC with  $S_{11}$  peak absorptions in a relatively blue wavelength region (well encapsulated with surfactants to have less SWCNT surface exposure to water media), their  $S_{11}$  peak absorbances generally remained the same but with varied optical density decrease amplitudes because of their differential protonation of SWCNT surfaces is considered as acid doping. It seems that the more negative  $\zeta$  potential of SWCNTs dispersed with such surfactant as 5% SC causes a smaller decrease in amplitude of  $S_{11}$  peak optical density. This implies that the more negative SWCNT surface  $\zeta$  potential prevented the attack of  $H^+$  to SWCNT, which has been considered as proton-mediated oxidation in literature. Additionally, the eluting strengths of different surfactant compositions for SWCNT separation using gel chromatography were examined by adding acids. Generally, the results show that SWCNTs dispersed in surfactants that are in an acidic condition could not be trapped in Sephacryl gels. In order to retain SWCNTs in gels, SWCNT solutions dispersed in surfactants need to be adjusted to basic conditions with high pH values.<sup>50</sup> Moreover, we expect that this contribution can cast light on the use of single-chirality SWCNT as a near-infrared probe for bioimaging and biosensing, for instance, as pH indicator in *in vitro* and *in vivo* experiments. Also, we expect this contribution can stimulate more fundamental researches on SWCNT spectroscopies, especially involving dipole moment

transition and symmetry selection, which seems to be missing in the literature.

## ASSOCIATED CONTENT

### Supporting Information

The Supporting Information is available free of charge on the ACS Publications website at DOI: 10.1021/acs.jpcc.8b10785.

Chemical structures of studied materials, all visible-near-infrared absorption spectra, and a photographic image of cloudy solution of (6,5) SWCNT after addition of 10  $\mu$ L of 5% HAc (PDF)

## AUTHOR INFORMATION

### Corresponding Author

\*(H.L.) E-mail: huaping.li@atomoe.com.

### ORCID

Huaping Li: 0000-0003-1285-4727

### Author Contributions

The manuscript was written through contributions of all authors. All authors have given approval to the final version of the manuscript.

### Notes

The authors declare no competing financial interest.

## ACKNOWLEDGMENTS

We are grateful to the generous financial support from Marine Corp System Command Office (Contract # M67854-17-C-6559). We also thank the reviewers for their invaluable suggestions and comments, and appreciate Professor Zhaohua Dai from Pace University for his diligent editions.

## ABBREVIATIONS

SWCNT, single-walled carbon nanotube; SDS, sodium dodecyl sulfate; SC, sodium cholate;  $S_{11}$ , the first Van Hove singularity transition; HAc, acetic acid; HCl, hydrochloric acid; NaOH, sodium hydroxide.

## REFERENCES

- (1) Yomogida, Y.; Tanaka, T.; Zhang, M.; Yudasaka, M.; Wei, W.; Kataura, H. Industrial-Scale Separation of High-Purity Single-Chirality Single-Wall Carbon Nanotubes for Biological Imaging. *Nat. Commun.* **2016**, *7*, 12056.
- (2) Heller, D. A.; Jin, H.; Martinez, B. M.; Patel, D.; Miller, B. M.; Yeung, T.-K.; Jena, P. V.; Höbartner, C.; Ha, T.; Silverman, S. K.; et al. Multimodal Optical Sensing and Analyte Specificity Using Single-Walled Carbon Nanotubes. *Nat. Nanotechnol.* **2009**, *4*, 114–120.
- (3) Zheng, Y.; Bachilo, S. M.; Weisman, R. B. Quenching of Single-Walled Carbon Nanotube Fluorescence by Dissolved Oxygen Reveals Selective Single-Stranded DNA Affinities. *J. Phys. Chem. Lett.* **2017**, *8*, 1952–1955.
- (4) Harvey, J. D.; Baker, H. A.; Mercer, E.; Budhathoki-Uprety, J.; Heller, D. A. Control of Carbon Nanotube Solvatochromic Response to Chemotherapeutic Agents. *ACS Appl. Mater. Interfaces* **2017**, *9*, 37947–37953.
- (5) Harvey, J. D.; Zerze, G. H.; Tully, K. M.; Mittal, J.; Heller, D. A. Electrostatic Screening Modulates Analyte Binding and Emission of Carbon nanotubes. *J. Phys. Chem. C* **2018**, *122*, 10592–10599.
- (6) Roxbury, D.; Jena, P. V.; Shamay, Y.; Horoszko, C. P.; Heller, D. A. Cell Membrane Proteins Modulate the Carbon Nanotube Optical Bandgap via Surface Charge Accumulation. *ACS Nano* **2016**, *10*, 499–506.

- (7) Zheng, M.; Diner, B. A. Solution Redox Chemistry of Carbon Nanotubes. *J. Am. Chem. Soc.* **2004**, *126*, 15490–1494.
- (8) Cathcart, H.; Nicolosi, V.; Hughes, J. M.; Blau, W. J.; Kelly, J. M.; Quinn, S. J.; Coleman, J. N. Ordered DNS Wrapping Switches on Luminescence in Single-Walled Nanotube Dispersions. *J. Am. Chem. Soc.* **2008**, *130*, 12734–12744.
- (9) Dukovic, G.; White, B. E.; Zhou, Z.; Wang, F.; Jockusch, S.; Steigerwald, M. L.; Heinz, T. F.; Friesner, R. A.; Turro, N. J.; Brus, L. E. Reversible Surface Oxidation and Efficient Luminescence Quenching in Semiconductor Single-Wall Carbon Nanotubes. *J. Am. Chem. Soc.* **2004**, *126*, 15269–15276.
- (10) Duque, J. G.; Densmore, C. G.; Doorn, S. K. Saturation of Surfactant Structure at the Single-Walled Carbon Nanotube Surface. *J. Am. Chem. Soc.* **2010**, *132*, 16165–16175.
- (11) Duque, J. G.; Oudjedi, L.; Crochet, J. J.; Tretiak, S.; Lounis, B.; Doorn, S. K.; Cognet, L. Mechanism of Electrolyte-Induced Brightening in Single-Wall Carbon Nanotubes. *J. Am. Chem. Soc.* **2013**, *135*, 3379–3382.
- (12) Niyogi, S.; Densmore, C. G.; Doorn, S. K. Electrolyte Tuning of Surfactant Interfacial Behavior for Enhanced Density-Based Separations of Single-Walled Carbon Nanotubes. *J. Am. Chem. Soc.* **2009**, *131*, 1144–1153.
- (13) Hirana, Y.; Tanaka, Y.; Niidome, Y.; Nakashima, N. Strong Micro-Dielectric Environment Effect on the Band Gaps of (n,m) Single-Walled Carbon Nanotubes. *J. Am. Chem. Soc.* **2010**, *132*, 13072–13077.
- (14) Larsen, B. A.; Deria, P.; Holt, J. M.; Stanton, I. N.; Heben, M. J.; Therien, M. J.; Blackburn, J. L. Effect of Solvent Polarity and Electrophilicity on Quantum Yields and Solvatochromic Shifts of Single-Walled Carbon Nanotube Photoluminescence. *J. Am. Chem. Soc.* **2012**, *134*, 12485–12491.
- (15) Wang, R. K.; Chen, W.-C.; Campos, D. K.; Ziegler, K. J. Swelling the Micelle Core Surrounding Single-Walled Carbon Nanotubes with Water-Immiscible Organic Solvents. *J. Am. Chem. Soc.* **2008**, *130*, 16330–16337.
- (16) Hirano, A.; Tanaka, T.; Urabe, Y.; Kataura, H. pH- and Solute-Dependent Adsorption of Single-Wall Carbon Nanotubes onto Hydrogels: Mechanistic Insights into the Metal/Semiconductor Separation. *ACS Nano* **2013**, *7*, 10285–10295.
- (17) Wang, L.; Li, Y. Selective Band Structure Modulation of Single-Walled Carbon Nanotubes in Ionic Liquids. *J. Am. Chem. Soc.* **2009**, *131*, 5364–5365.
- (18) Salem, D. P.; Gong, X.; Liu, A. T.; Koman, V. B.; Dong, J.; Strano, M. S. Ionic Strength-Mediated Phase Transitions of Surface-Adsorbed DNA on Single-Walled Carbon Nanotubes. *J. Am. Chem. Soc.* **2017**, *139*, 16791–16802.
- (19) Ding, J.; Li, Z.; Lefebvre, J.; Du, X.; Malenfant, R. L. Mechanistic Consideration of pH Effect on the Enrichment of Semiconducting SWCNTs by Conjugated Polymer Extraction. *J. Phys. Chem. C* **2016**, *120*, 21946–21954.
- (20) Nakayama-Ratchford, N.; Bangsaruntip, S.; Sun, X.; Welsher, K.; Dai, H. Noncovalent Functionalization of Carbon Nanotubes by Fluorescein-Polyethylene Glycol: Supramolecular Conjugates with pH-Dependent Absorbance and Fluorescence. *J. Am. Chem. Soc.* **2007**, *129*, 2448–2449.
- (21) Strano, M. S.; Huffman, C. B.; Moore, V. C.; O'Connell, M. J.; Haroz, E. H.; Hubbard, J.; Miller, M.; Rialon, K.; Kittrell, C.; Ramesh, S.; et al. Reversible, band-Gap-Selective Protonation of Single-Walled Carbon Nanotubes in Solution. *J. Phys. Chem. B* **2003**, *107*, 6979–6985.
- (22) Blackburn, J. L.; McDonald, T. J.; Metzger, W. K.; Engtrakul, C.; Rumbles, G.; Heben, M. J. Protonation Effects on the Branching Ratio in Photoexcited Single-Walled Carbon Nanotube Dispersions. *Nano Lett.* **2008**, *8*, 1047–1054.
- (23) Wang, D.; Chen, L. Temperature and pH-Responsive Single-Walled Carbon Nanotube Dispersions. *Nano Lett.* **2007**, *7*, 1480–1484.
- (24) Moonosawmy, K. R.; Kruse, P. Cause and Consequence of Carbon Nanotube Doping in Water and Aqueous Media. *J. Am. Chem. Soc.* **2010**, *132*, 1572–1577.
- (25) Rohlfling, M. Redshift of Excitons in Carbon Nanotubes Caused by the Environment Polarizability. *Phys. Rev. Lett.* **2012**, *108*, 087402.
- (26) Berger, S.; Iglesias, F.; Bonnet, P.; Voisin, C.; Cassabois, G.; Lauret, J.-S.; Delalande, C.; Roussignol, P. Optical Properties of Carbon Nanotubes in a Composite Material: the Role of Dielectric Screening and Thermal Expansion. *J. Appl. Phys.* **2009**, *105*, 094323.
- (27) Hirano, A.; Tanaka, T.; Kataura, H. Thermodynamic Determination of the Metal/Semiconductor Separation of Carbon Nanotubes Using Hydrogels. *ACS Nano* **2012**, *6*, 10195–10205.
- (28) Liu, H.; Tanaka, T.; Urabe, Y.; Kataura, H. High-Efficiency Single-Chirality Separation of Carbon Nanotubes Using Temperature-Controlled Gel Chromatography. *Nano Lett.* **2013**, *13*, 1996–2003.
- (29) Moore, V. C.; Strano, M. S.; Haroz, E. H.; Hauge, R. H.; Smalley, R. E.; Schmidt, J.; Talmon, Y. Individually Suspended Single-Walled Carbon Nanotubes in Various Surfactants. *Nano Lett.* **2003**, *3*, 1379–1382.
- (30) Choi, J. H.; Strano, M. S. Solvatochromism in Single-Walled Carbon Nanotubes. *Appl. Phys. Lett.* **2007**, *90*, 223114.
- (31) Strano, M. S.; Moore, V. C.; Miller, M. K.; Allen, M. J.; Haroz, E. H.; Kittrell, C.; Hauge, R. H.; Smalley, R. E. The Role of Surfactant Adsorption During Ultrasonication in the Dispersion of Single-Walled Carbon Nanotubes. *J. Nanosci. Nanotechnol.* **2003**, *3*, 81–86.
- (32) Silvera-Batista, C. A.; Wang, R. K.; Weinberg, P.; Ziegler, K. J. Solvatochromic Shifts of Single-Walled Carbon Nanotubes in Nonpolar Microenvironments. *Phys. Chem. Chem. Phys.* **2010**, *12*, 6990–6998.
- (33) Zhou, L. L.; Liu, X.; Li, H. P. The Release of Retained Single-Walled Carbon Nanotubes in Gels. *Langmuir* **2018**, *34*, 12224–12232.
- (34) McRae, E. G. Theory of Solvent Effects on Molecular Electronic Spectra. Frequency Shifts. *J. Phys. Chem.* **1957**, *61*, 562–572.
- (35) Nagae, H. Theory of Solvent Effects on Electronic Absorption Spectra of Rodlike or Disklike Solute Molecules: Frequency Shifts. *J. Chem. Phys.* **1997**, *106*, 5159–5170.
- (36) Blanch, A. J.; Quinton, J. S.; Shapter, J. G. The Role of Sodium Dodecyl Sulfate Concentration in the Separation of Carbon Nanotubes Using Gel Chromatography. *Carbon* **2013**, *60*, 471–480.
- (37) Blanch, A. J.; Shapter, J. G. Surfactant Concentration Dependent Spectral Effects of Oxygen and Depletion Interactions in Sodium Dodecyl Sulfate Dispersions of Carbon Nanotubes. *J. Phys. Chem. B* **2014**, *118*, 6288–6296.
- (38) Ju, S.-Y.; Kopcha, W. P.; Papadimitrakopoulos, F. Brightly Fluorescent Single-Walled Carbon nanotubes via An Oxygen-Excluding Surfactant Organization. *Science* **2009**, *323*, 1319–1323.
- (39) Li, H. P.; Liu, H. Y.; Tang, Y. F.; Guo, W. M.; Zhou, L. L.; Smolinski, N. Electronically Pure Semiconducting Single-Walled Carbon Nanotube for Large Scale Electronic Devices. *ACS Appl. Mater. Interfaces* **2016**, *8*, 20527–20533.
- (40) Li, H. P.; Tang, Y. F.; Guo, W. M.; Liu, H. Y.; Zhou, L. L.; Smolinski, N. Polyfluorinated Electrolyte for Fully Printed Carbon Nanotube Electronics. *Adv. Funct. Mater.* **2016**, *26*, 6914–6920.
- (41) Acetic Acid in Wikipedia homepage. [https://en.wikipedia.org/wiki/Acetic\\_acid/](https://en.wikipedia.org/wiki/Acetic_acid/) (accessed December 8, 2018).
- (42) Chakraborty, S.; Shukla, D.; Jain, A.; Mishra, B.; Singh, S. Assessment of Solubilization Characteristics of Different Surfactants for Carvedilol Phosphate As A Function of pH. *J. Colloid Interface Sci.* **2009**, *335*, 242–249.
- (43) Cholic Acid in Drugbank homepage. <https://www.drugbank.ca/drugs/DB02659/> (accessed December 8, 2018).
- (44) Li, H. P.; Zhou, L. L. Visualizing Helical Wrapping of Semiconducting Single-Walled Carbon Nanotubes by Surfactants and Their Impacts on Electronic Properties. *Chem. Select* **2016**, *1*, 3569–3572.

(45) White, B.; Banerjee, S.; O'Brien, S.; Turro, N. J.; Herman, I. P. Zeta-Potential Measurements of Surfactant-Wrapped Individual Single-Walled Carbon Nanotubes. *J. Phys. Chem. C* **2007**, *111*, 13684–13690.

(46) Sun, Z.; Nicolosi, V.; Rickard, D.; Bergin, S. D.; Aherne, D.; Coleman, J. N. Quantitative Evaluation of Surfactant-stabilized Single-walled Carbon Nanotubes: Dispersion Quality and Its Correlation with Zeta Potential. *J. Phys. Chem. C* **2008**, *112*, 10692–10699.

(47) Shastry, T. A.; Morris-Cohen, A. J.; Weiss, E. A.; Hersam, M. C. Probing Carbon Nanotube–Surfactant Interactions with Two-Dimensional DOSY NMR. *J. Am. Chem. Soc.* **2013**, *135*, 6750–6753.

(48) Oh, H.; Sim, J.; Ju, S.-Y. Binding Affinities and Thermodynamics of Noncovalent Functionalization of Carbon Nanotubes with Surfactants. *Langmuir* **2013**, *29*, 11154–11162.

(49) Flavel, B. S.; Kappes, M. M.; Krupke, R.; Hennrich, F. Separation of Single-Walled Carbon Nanotubes by 1-Dodecanol-Mediated Size-Exclusion Chromatography. *ACS Nano* **2013**, *7*, 3557–3564.

(50) Zeng, X.; Yang, D.; Liu, H.; Zhou, N.; Wang, Y.; Zhou, W.; Xie, S.; Kataura, H. Detecting and Tuning the Interactions Between Surfactants and Carbon Nanotubes for Their High Efficiency Structure Separation. *Adv. Mater. Interfaces* **2018**, *5*, 1700727.